

1997

19980803 081

ADAPTIVE OBSERVATIONS IN FASTEX IOP-18: DATA IMPACT AND SYNOPTIC INTERPRETATION

ROLF H. LANGLAND, RONALD GELARO, GREGORY D. ROHALY

Naval Research Laboratory, Monterey, California, USA

MELVYN A. SHAPIRO

NOAA/ETL, Boulder, Colorado, USA

1. INTRODUCTION

An issue of major importance in numerical weather prediction is the requirement to provide models with accurate initial conditions. The Fronts and Atlantic Storm Track Experiment (FASTEX) provides an opportunity to examine the impact of special observational data in 1-3 day forecasts of north Atlantic cyclones. An overview of FASTEX objectives and observational resources is contained in Joly et al (1997). The FASTEX field phase (January - February 1997) provided the first test of so-called "adaptive" observation techniques, in which objective guidance from numerical models was used to "target" observational resources (e.g., dropsonde aircraft) to specific areas. In this study we describe the impact of targeted aircraft dropsonde, and GOES-8 wind data on a 24 hr forecast of the cyclone in FASTEX IOP-18.

It is well-established that numerical forecasts are much more sensitive to initial condition changes in certain locations than in others. In "sensitive" locations, changes to initial conditions (*including changes which might result from new observational data*) can have critical effects on the development of a forecast feature, such as a cyclone, or on measures of forecast error. Adjoint methods can be used to determine sensitivity patterns related to error growth in mid-latitude forecast situations, (for example, see Rabier et al. 1996). Both dry and moist adjoint sensitivity studies suggest that mid-latitude synoptic-scale cyclones (on the 1-3 day range) have maximum sensitivity to temperature and wind in the mid-lower troposphere (roughly 400-800 mb), in relatively localized areas of the upstream baroclinic storm track (also see Langland et al. 1995).

The problem of adaptive observations does not center on identifying and correcting the largest analysis errors, but rather on correcting analysis error in critical locations, where any initial error can amplify with very large growth rates. A practical strategy for best use of observational resources is to focus on locations that are dynamically sensitive, using adjoint-derived singular vectors and sensitivity, which can be provided in an operational time-frame.

A primary platform for targeted observations in FASTEX was the NOAA Gulfstream-IV (G-IV) aircraft, which provides dropsonde temperature, wind, and moisture observations. The G-IV dropsonde data do not, by themselves, provide adequate coverage of the upstream observational target areas in FASTEX, because of various logistical constraints during the field program. For this reason, we supplement the G-IV dropsonde data with satellite-derived cloud track and water vapor winds (Velden et al. 1997). The satellite winds are useful: a) to provide supplemental data in areas of the target not covered by aircraft dropsondes, and b) to provide data in "null" (non-sensitive) areas for verification of the targeting strategies. In addition, the impact of the satellite data by itself is of great interest, since GOES-8 and -9 provide a regular source of high-quality wind observations, which are currently underutilized by operational forecast models

2. TARGETING PROCEDURE

We select IOP-18 as a case which provides perhaps the best G-IV dropsonde coverage of an adjoint-based observational target area in FASTEX. The model used is the Navy Operational Global Atmospheric Prediction System (NOGAPS) run at T79L18, and its (dry) tangent linear and adjoint, also run at T79L18, to provide singular vectors. A "control" 24 hr model run is made from initial conditions at Feb 22/12 UTC which are developed from a 6 hr assimilation cycle (multivariate OI) that contains no special FASTEX aircraft, ship, or radiosonde data during the previous 24 hr. The 24 hr control forecast of sea level pressure is depicted in Fig. 1a. We attempt to reduce the 8 mb forecast error of the control run (Fig. 1b) by assimilating G-IV dropsonde data (surface-27,000 ft, 10-14 UTC) and GOES-8 winds (250-900 mb, 11-13 UTC) in target areas of strong sensitivity at Feb 22/12 UTC. The verifying analysis at Feb 23/12 UTC includes some supplemental FASTEX data. The observed cyclone deepens from 984 to 958 mb during the 24 hr interval.

Fig. 2 shows the vorticity component of singular vector (SV) #1 at 310 and the temperature component of SV #3 at 760 mb, valid at Feb 22/12 UTC. These singular vectors use a total energy norm at initial (target) time, Feb 22/12 UTC and final (verification) time, Feb 23/12 UTC. The cyclone verification area is 48-63N,

15-30W, and from 150 mb to the surface. The singular vector calculation was started from Feb 21/12 UTC, to allow time for the G-IV to be deployed to the target area from its base in Shannon, Ireland. The primary observational target area (45-58N, 30-55W) is identified to include the area in which the leading singular vectors have largest amplitude at initial time, considering both temperature and vorticity components (Fig. 2). Areas of large SV amplitude extending over eastern Canada were considered less likely to require special observations due to proximity of land-based observations.

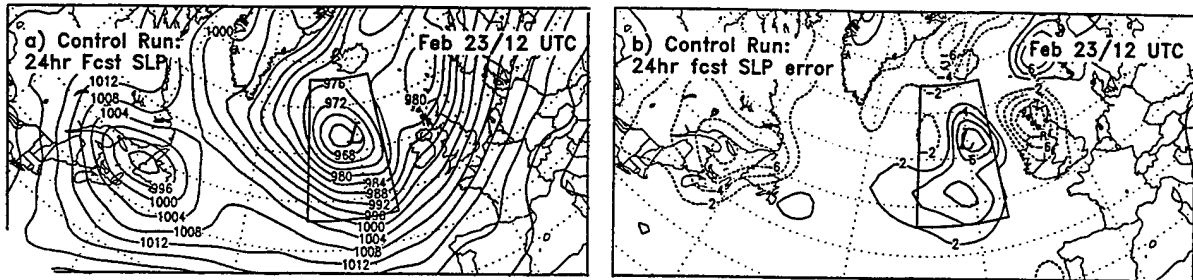


Fig. 1: Sea-level pressure (mb): a) 24 hr "control" forecast, valid at Feb 23/12 UTC 1997; b) error of the control forecast. Solid line (box) in b) defines verification area used for adjoint calculations. *L* is observed surface cyclone position at Feb 23/12 UTC (verify time).

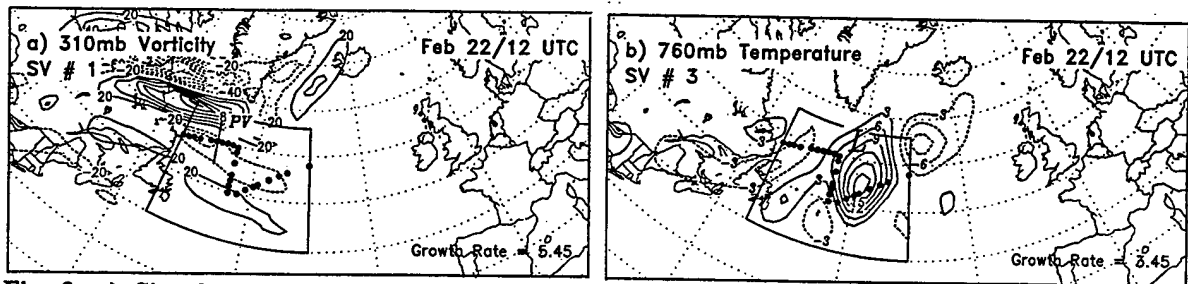


Fig. 2: a) Singular vector #1 vorticity component at 310 mb; b) Singular vector #3 temperature component at 760 mb. Valid at Feb 22/12 UTC 1997. Solid line (box) is observational target area for G-IV dropsondes (solid dots). *L* is observed surface cyclone position at Feb 22/12 UTC (target time).

3. IMPACT OF TARGETED DATA

The increment of 760 mb temperature resulting from assimilation of the G-IV dropsondes is depicted in Figs. 3a. It is evident that these analysis temperature corrections at 760 mb, which are primarily in the cyclone warm sector, project strongly onto the SV structure depicted in Fig. 2b. However, the analysis corrections of upper level (310 mb) vorticity (not shown) project onto a more weakly growing part of the singular vector structure near 54N, 48W (Fig. 2a). Assimilation of the G-IV data produces a 6 mb change to the 24 hr sea-level pressure (SLP) forecast (Fig. 3b), just south of the verifying cyclone position. When GOES-8 winds are also assimilated, a somewhat better fit to the spatial pattern of forecast error is obtained (not shown), and the magnitude of change to 24 hr SLP is similar to the G-IV-only case.

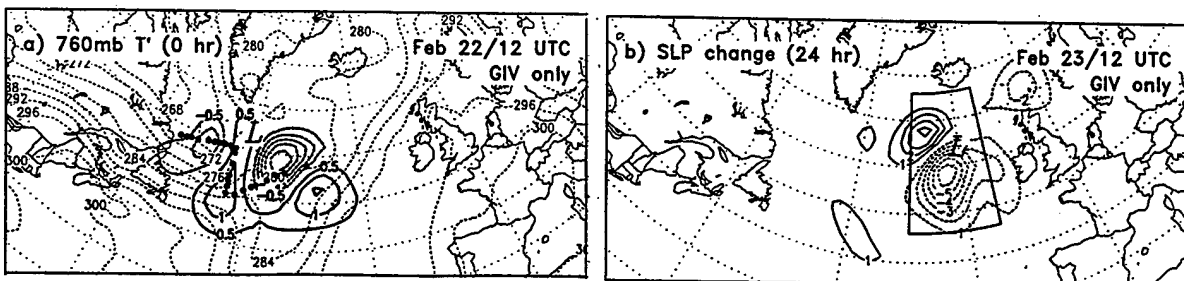


Fig. 3: a) Analysis increment (G-IV - control) of 760 mb temperature (bold contours, °C) at Feb 22/12 UTC 1997; b) the change in 24 hr forecast SLP (mb) valid at Feb 23/12 UTC due to assimilation of G-IV dropsondes. Light dashed contours in a) are 760 mb potential temperature (K). Solid line (box) in b) is cyclone verification area. *L* is observed surface cyclone position.

An indication of forecast improvement is provided by change to a quantitative measure of forecast error in the verification region (48-63N, 15-30W). The measures used are

$$\varepsilon_{24} = \langle e_{24}; E e_{24} \rangle$$

$$\Delta \varepsilon_{24} = \frac{\varepsilon_{24}^{(exp)} - \varepsilon_{24}^{(cntrl)}}{\varepsilon_{24}^{(cntrl)}}$$

where ε_{24} is the forecast energy norm, e_{24} is the model state vector 24 hr forecast error, E is a matrix of energy weights, and $\Delta \varepsilon_{24}$ is the percent change in the norm in a new forecast (*exp*) with respect to the control (*cntrl*) forecast.

Initial Conditions	ε_{24} (m ² s ⁻²)	$\Delta \varepsilon_{24}$ (%)
Control	0.1717	---
G-IV	0.1284	-25
G-IV+GOES/Target	0.1065	-38
GOES-8 Null	0.1686	-2

Table 1: Initial condition impact on the forecast error norm: FASTEX IOP-18, Feb 22/12 UTC - Feb 23/12 UTC 1997. Computed at T79 resolution.

Inclusion of only the G-IV dropsonde data reduces the forecast energy norm by 25 percent (Table 1). The best result (38 percent reduction) is obtained from a combined assimilation of G-IV dropsondes and GOES-8 winds over a large "target" area (45-65N, 10-70W). Assimilation of GOES-8 winds in "null" areas of weak sensitivity (outside of 45-65N, 40-70W) reduces the forecast energy norm by only 2 percent.

The results of this study suggest that adjoint singular vector and sensitivity information derived in real-time can provide useful guidance for adaptive observations in forecasts of extratropical cyclones, even though approximations and assumptions are involved in the adjoint targeting procedures. The assimilation of aircraft dropsonde and satellite wind data suggests that correction of analysis errors in the mid-low tropospheric cyclone warm sector can be an important factor in forecast skill improvements.

4. REFERENCES

- Joly, A, D Jorgensen, M A Shapiro, A Thorpe, P Bessemoulin, K A Browning, J-P Cammas, J-P Chalon, S A Clough, K A Emanuel, L Eymard, R Gall, P H Hildebrand, R H Langland, Y Lemaitre, P Lynch, J A Moore, P O G Persson, C Snyder and R M Wakimoto, 1997: The Fronts and Atlantic Storm-Track Experiment (FASTEX): Scientific Objectives and Experimental Design, 1997: *Bull. Am. Met. Soc.*, 78, 1917-1940.
- Langland, R H, R L Elsberry and R M Errico, 1995: Evaluation of physical processes in an idealized extratropical cyclone using adjoint sensitivity. *Q. J. R. Meteorol. Soc.*, 121, 1349-1386.
- Rabier, F, E Klinker, P Courtier and A Hollingsworth, 1996: Sensitivity of forecast errors to initial conditions. *Q. J. R. Meteorol. Soc.*, 122, 121-150.
- Velden, C S, C M Hayden, S J Nieman, W P Menzel, S Wanzong and J S Goerss, 1997: Upper tropospheric winds derived from geostationary satellite water vapor observations. *Bull. Am. Met. Soc.*, 78, 173-195.
- Acknowledgment:** The authors thank Thomas Rosmond for providing the NOGAPS adjoint code used for these studies, and Chris Velden for providing GOES-8 winds. The research was partially supported by ONR program element PE0601153N.